Published in final edited form as:
J Am Chem Soc. 2012 March 14; 134(10): 4545–4548. doi:10.1021/ja300276s.

Induction of pH sensitivity on the fluorescence lifetime of quantum dots by NIR fluorescent dyes

Rui Tang, **Hyeran Lee**, and **Samuel Achilefu***
Department of Radiology, Washington University, St. Louis, Missouri 63110, United States

Abstract

Modulation of the fluorescence lifetime (FLT) of CdTeSe/ZnS quantum dots (QDs) by near-infrared (NIR) organic chromophores represents a new strategy to generate reproducible pH-sensing nanomaterials. The hybrid construct transfers the pH-sensitivity of photo-labile NIR cyanine dyes to highly emissive and long lifetime pH-insensitive QDs, thereby inducing reproducible FLT change from 29 ns at pH >7 to 12 ns at pH <5. This approach provides an unparalleled large dynamic FLT range for pH sensing in the NIR wavelengths.

Keywords

Near infrared; quantum dot; pH sensitive; fluorescence lifetime; optical imaging; nanoparticles

Fluorescent molecular probes are useful for sensing many chemical and biological processes, such as pH, ligand binding, enzyme activity, and salt concentrations.[1–3] Because of the critical roles acidity of mediums play in biological systems,[4,5] a variety of intracellular pH reporting strategies with organic dyes have been developed.[6] Recent efforts to translate findings in cell assays to living organisms have led to concerted efforts to develop pH-sensitive near-infrared (NIR) molecular probes and nanoparticles for assessing the functional status of both cells and tissue.[7–10] These sensors relied on fluorescence intensity measurements using a reference calibration model or ratiometric fluorescence techniques. The inherent difficulties with reproducibility of intensity measurements and the complexity of implementing quantitative in vivo measurements with emissions at disparate wavelengths (typically in the visible and NIR regions) have increased interest in the use of fluorescence lifetime (FLT) technique for pH sensing because FLT is less dependent on several factors that perturb intensity measurements.[11–13]

Despite these advances, changes in the FLT of NIR organic fluorophores in response to pH are marginal. Reported FLT changes between acidic and basic mediums are <1 ns. Another major limitation of using NIR organic dyes as pH sensors for intracellular pH measurements is the poor photostability, which is amplified in FLT techniques, where longer signal integration time is typically needed. An alternative approach is to use semiconductor quantum dots (QDs), which offer significant advantages over conventional organic dyes. These include broad absorption spectrum for flexibility in excitation wavelengths; large multiphoton action cross sections for efficient multiphoton microscopy; narrow, sizetunable emission for multicolor imaging; superior photostability for longitudinal studies; high quantum yield for improving detection sensitivity; and long fluorescence lifetime to

Corresponding Author, achilefus@mir.wustl.edu.

ASSOCIATED CONTENT

Supporting Information. Detailed experimental methods, dye structures, spectral properties of different constructs, de-convolution of the spectra and pKa measurements are provided. These materials are available free of charge via the Internet at http://pubs.acs.org.

minimize interference from naturally occurring organic fluorophores.[14–19] Although the intrinsic spectral insensitivity of the QDs to the environmental changes favors reproducibility of fluorescence data, surface coatings or labeling have been shown to alter their spectral properties.[20] This feature has been used to develop biosensors, where QD fluorescence intensity is modulated by organic molecules through energy or electron transfer processes.[21–27] Most of these studies are based on visible light-emitting QDs and relied on spectral shifts or luminescence intensity changes. Despite the enormous progress made with these hybrid nanomaterials, the need for NIR pH sensors with large dynamic measurement parameters for in vitro, cellular, and in vivo applications remains unmet.

Our goal in this study is to develop a general strategy for generating photostable NIR pH sensors with large dynamic pH-sensing capability. The hybrid constructs incorporates the excellent photophysical properties of QDs with the high pH sensitivity of NIR organic dyes. Inversion of pH response can be achieved by switching from Förster resonance energy transfer (FRET) to photoinduced electron transfer (PET) quenching processes.

We first prepared the NIR pH-sensitive carbocyanine dye, LS662 (Scheme 1), by the method described previously.[7] LS662 exhibits absorption maxima in the NIR (750 nm) at low pH, but gives a hypsochromic shift to the visible region (520 nm) as pH increases, with a pKa of 5.2 (Figure S1). Above pH 7, the dye fluorescence was insignificant. The dye itself is not suitable for FLT pH measurement because of its <0.2 ns FLT change in the physiologic useful pH range of 4–7. However, these spectral properties are suitable for developing FRET-based QD pH sensors by modulating the emission properties of QD at either 500 nm or 750 nm with LS662.

CdTeSe QDs coated with ZnS and capped with cysteamine were synthesized and further conjugated to LS662 (Scheme 1). The hybrid nanomaterials were purified by either dialysis or centrifugation, followed by removal of the supernatant. (see SI for detailed synthesis procedures and characterization of CdTeSe/ZnS QDs and the QD-organic dye conjugates). The cysteamine ligands served as amine reactive functionality and aided the stabilization and solubility of the colloidal QDs in aqueous medium across a wide pH range.

Transmission electronic microscopy (TEM) of QD-dye conjugates showed an average diameter of 9.4 nm, with fairly monodispersed distribution (Figure 1A,B). Both organic surface ligands and conjugated dye molecules increased the QD hydrodynamic diameter to ~18.2 nm (Figure 1C), as determined by dynamic light scattering (DLS). Based on the de-convolution of the absorption spectra of the QD-dye, a 1:8 QD:dye ratio was calculated (Figure S4).

To accurately report dye-modulated pH response, the QDs and the surface coatings should lack inherent pH sensitivity and have luminescence at about 520 nm or 750 nm to match the spectral shift of LS662. Spectral analysis showed that the luminescence intensity of the parent cysteamine-coated CdTeSe/ZnS QD750 lacks pH-sensitivity (Figure S2). In contrast, the QD-dye conjugate revealed a biphasic absorption response to pH (Figure 2A). Unlike LS662, which exhibited an inverse relationship with pH increase at 770 nm, the luminescence of QD750 in QD750-LS662 increased with increase in pH at 750 nm (Figure 2B).

Because FRET efficiency is determined by the extent of spectral overlap between the QD emission and the dye absorption, pH-dependent spectral shifts of dye absorption results in the alteration of FRET efficiency. Based on the spectral properties of LS662, QD750 luminescence has excellent spectral overlap with the dye's NIR absorption at low pHs. This allows energy transfer from the QD to the dye molecules, resulting in the quenching of QD emission. Additional quenching could be induced by PET from the dye's tertiary amine to

the QD.[28] The expected shift in the dye's absorption from 750 nm to 520 nm under basic pH produced high QD750 luminescence (Figure 2). The small Stokes shift of the NIR dye, coupled with a significant overlap of its fluorescence with QD750 emission, complicates determination of the energy transfer efficiency (E) by changes in fluorescence intensity. However, this parameter could be determined by FLT measurements.

Toward this goal, we explored the FLT-based pH sensitivity of the QD-dye conjugate in different buffer solutions. FLT of the QDs alone has a small FLT pH response between 29 ns and 31 ns (Figure S2C). This narrow FLT change represents <10% of the native QD FLT, and does not have the dynamic FLT range for pH sensing in heterogeneous mediums. In contrast, the FLT decay profile of QD-dye conjugate at 750 nm emission showed significant pH response (Figure 3A), decreasing from 29 ns at pH >7 to 12 ns at pH <5. A plot of the FLT vs. pH showed a sigmoidal transition with a pKa of 5.2 (Figure 3B). This pKa mirrored that of the dye using fluorescence intensity measurement, but with a reversal of the intensity vs. pH response (Figure S1). This demonstrates that the organic dye imparted its pH sensitivity to QDs with high accuracy, and provides a general strategy to improve the photostability and signal dynamic range of organic pH-sensitive molecules.

To determine the FRET efficiency (*E*) by FLT, we used the equation, $E=1-\tau_a/\tau_b$, where τ_a is 12 ns (the QD750 FLT at pH 2 - all dye absorption overlaps with QD emission) and τ_b is 29 ns (determined at pH 10 - no dye absorption overlap with QD750 emission). On this basis, the FRET efficiency of ~60% was determined at the two extreme pH states. This validates the choice of FLT instead of emission intensity as pH reporting parameter. At 60%, residual QD emission is still significant, and without a ratiometric strategy, quantitative pH measurement in cells and tissue would otherwise be complicated.

A potential strategy to incorporate ratiometric pH sensing is to label two different QDs emitting at 520 nm and 750 nm with LS662 to match the absorption shift of the dye at different pH. Thus, we prepared QD560-LS662, which was designed to have spectra overlap with LS662 absorption in neutral to basic pH mediums (Figure S5A). As expected, FRET efficiency of this construct increases as pH increases, resulting in a reversed FLT trend compared to that of QD750-LS662 (Figure S5B,C). The QD560-LS662 also showed a significant FLT change at 560 nm emission from 7 ns at pH >7 to 31 ns at pH <5, with a pKa of 5.5 and FRET efficiency of ~77% between pH 2 (31 ns) and pH 10 (7 ns). Thus, FLT alone or ratiometric pH measure with combined QD560-LS662 and QD750-LS662 can successfully be used to determine quantitatively the pH of chemical and biological systems.

To validate that the induction of the pH-sensitivity on the QDs originated from pH-sensitive organic dye, we conjugated QD750 to a non-pH sensitive dye, LS288 (Figure S8). This dye has an absorption and emission maxima at 760 nm and 780 nm, respectively. The photophysical properties of this dye, including absorption, emission and fluorescence lifetime of QD750-LS288 construct were investigated at different pH values (Figure S6). Upon conjugation of the dye to QD750, a significant pH-independent emission quenching occurred, resulting in *E* of ~73% at all pH values between 2 and 10. Here, *E* was determined by defining τ_a and τ_b as the FLT after (7 ns) and before (26 ns) dye conjugation. This finding could be used to develop stable activatable probes that will restore QD fluorescence after removal of the non-pH sensitive dye by enzymes or other biological events. More importantly, the result confirms the role of organic pH dyes in imparting pH sensitivity to QDs.

To explore the generality of the pH sensing strategy, we prepared a pH-sensitive heptamethine dye LS664, which fluoresces in acidic environment, but quenches fluorescence by PET mechanism under neutral and basic conditions (Scheme 1 and Figure

S7). This dye has absorption maxima of 760 nm below pH 4, which shifts to 810 nm above pH 5, generating the nonfluorescent analogue. Both absorption and emission spectral analyses at different pH values gave pKa of 3.2. Using a similar method described for the synthesis of QD750, we prepared cysteamine coated CdTeSe/ZnS QD emitting at 760 nm (QD760, Figure S9) to overlap with the absorption maxima of LS664 under acidic conditions. The QD-dye conjugate, QD-dye (QD760-LS664) was prepared and its pH-dependent FLT response was investigated (Figure 4). If FRET was the primary quenching mechanism, we would expect QD emission quenching at pH <4 and significant emission intensity at pH>5. Instead, the QD emission quenching increased with pH, as reflected by the FLT plot (Figure 4). The mechanism of luminescence quenching and enhancement by LS664 is not fully understood at this time, but previous studies have shown that amines are electron donors to QDs and could be involved in PET mediated QD emission quenching.[28] Although QD760 is coated with cysteinamine, which could serve as electron donor under basic conditions, we did not observe PET with the analogous QD750. Since the major difference between the two QD formulations are the dyes, we attribute this quenching to PET from the amine groups on the indolium ring of LS664 to the QD under basic conditions. The obtained pKa value from the sigmoidal fit of the lifetime decay profile is 3.5, which is also consistent with the pKa of LS664 alone. This demonstrates the feasibility of applying pH-sensitive dyes with PET capability to modulate the FLT of QDs. However, delineation of the exact process by which LS664 perturbs the spectral properties of QD needs further exploration.

In summary, we have developed new pH-sensitive QD-organic dye hybrid nanomaterials by imparting the pH-sensing properties of NIR dyes to photostable QDs possessing large FLT sensitivity scale. In particular, perturbation of the QD's FLT by FRET or PET processes illustrates the generality of the approach. The QD FRET donors are readily custom-engineered to match the acceptor's absorption features of a pH sensitive dye used to modulate the FLT of QDs. This new approach allows environmentally insensitive QDs to become highly efficient pH sensors for a variety of potential environmental and biological applications. For example, the large two-photon (2P) action cross sections of QDs and the deep tissue penetration NIR light ideally position these sensors for use in multiphoton microscopy of molecular processes across large spatial scales ranging from cells to thick tissue. Moreover, direct 2P excitation of the highly photostable QDs prevents the rapid photobleaching of the NIR pH-sensitive cyanine dyes, which readily occurs under high intensity lasers."

Supplementary Material

Refer to Web version on PubMed Central for supplementary material.

Acknowledgments

Funding Sources

This study is based upon work supported in part by the NIH grants R01 EB007276, R01 EB008111, R33 CA123537, U54 CA136398 – Network for Translational Research, and HHSN268201000046C – NHLBI Program of Excellence in Nanotechnology.

REFERENCES

1. Dahan M, Levi S, Luccardini C, Rostaing P, Riveau B, Triller A. Science. 2003; 302:442. [PubMed: 14564008]
2. Michalet X, Pinaud FF, Bentolila LA, Tsay JM, Doose S, Li JJ, Sundaresan G, Wu AM, Gambhir SS, Weiss S. Science. 2005; 307:538. [PubMed: 15681376]

3. Lidke DS, Nagy P, Heintzmann R, Arndt-Jovin DJ, Post JN, Grecco HE, Jares-Erijman EA, Jovin TM. Nat Biotechnol. 2004; 22:198. [PubMed: 14704683]
4. Casey JR, Grinstein S, Orlowski J. Nat Rev Mol Cell Biol. 2010; 11:50. [PubMed: 19997129]
5. Srivastava J, Barber DL, Jacobson MP. Physiology (Bethesda). 2007; 22:30. [PubMed: 17289928]
6. Han J, Burgess K. Chem Rev. 2010; 110:2709. [PubMed: 19831417]
7. Lee H, Akers W, Bhushan K, Bloch S, Sudlow G, Tang R, Achilefu S. Bioconjug Chem. 2011; 22:777. [PubMed: 21388195]
8. Hilderbrand SA, Kelly KA, Niedre M, Weissleder R. Bioconjug Chem. 2008; 19:1635. [PubMed: 18666791]
9. Patonay G, Casay GA, Lipowska M, Strekowski L. Talanta. 1993; 40:935. [PubMed: 18965731]
10. Chen Y, Li X. Biomacromolecules. 2011; 12:4367. [PubMed: 22040128]
11. Povrozin YA, Markova LI, Tatarets AL, Sidorov VI, Terpetschnig EA, Patsenker LD. Anal Biochem. 2009; 390:136. [PubMed: 19351524]
12. Berezin MY, Guo K, Akers W, Northdurft RE, Culver JP, Teng B, Vasalatiy O, Barbacow K, Gandjbakhche A, Griffiths GL, Achilefu S. Biophys J. 2011; 100:2063. [PubMed: 21504743]
13. Almutairi A, Guillaudeu SJ, Berezin MY, Achilefu S, Frechet JM. J Am Chem Soc. 2008; 130:444. [PubMed: 18088125]
14. Murray CB, Norris DJ, Bawendi MG. J Am Chem Soc. 1993; 115:8706.
15. Parak WJ, Gerion D, Pellegrino T, Zanchet D, Micheel C, Williams SC, Boudreau R, Le Gros MA, Larabell CA, Alivisatos AP. Nanotechnology. 2003; 14:R15.
16. Clapp AR, Medintz IL, Mauro JM, Fisher BR, Bawendi MG, Mattoussi H. J Am Chem Soc. 2004; 126:301. [PubMed: 14709096]
17. Medintz IL, Konnert JH, Clapp AR, Stanish I, Twigg ME, Mattoussi H, Mauro JM, Deschamps JR. Proc Natl Acad Sci U S A. 2004; 101:9612. [PubMed: 15210939]
18. Murphy CJ. Anal Chem. 2002; 74:520A.
19. Dabbousi BO, RodriguezViejo J, Mikulec FV, Heine JR, Mattoussi H, Ober R, Jensen KF, Bawendi MG. Journal of Physical Chemistry B. 1997; 101:9463.
20. Medintz IL, Stewart MH, Trammell SA, Susumu K, Delehanty JB, Mei BC, Melinger JS, Blanco-Canosa JB, Dawson PE, Mattoussi H. Nat Mater. 2010; 9:676. [PubMed: 20651808]
21. Tomasulo M, Yildiz I, Raymo FM. J Phys Chem B. 2006; 110:3853. [PubMed: 16509664]
22. Snee PT, Somers RC, Nair G, Zimmer JP, Bawendi MG, Nocera DG. J Am Chem Soc. 2006; 128:13320. [PubMed: 17031920]
23. Mattoussi H, Mauro JM, Goldman ER, Anderson GP, Sundar VC, Mikulec FV, Bawendi MG. J Am Chem Soc. 2000; 122:12142.
24. Bruchez M, Moronne M, Gin P, Weiss S, Alivisatos AP. Science. 1998; 281:2013. [PubMed: 9748157]
25. Chan WC, Nie S. Science. 1998; 281:2016. [PubMed: 9748158]
26. Goldman ER, Anderson GP, Tran PT, Mattoussi H, Charles PT, Mauro JM. Anal Chem. 2002; 74:841. [PubMed: 11866065]
27. Goldman ER, Medintz IL, Whitley JL, Hayhurst A, Clapp AR, Uyeda HT, Deschamps JR, Lassman ME, Mattoussi H. J Am Chem Soc. 2005; 127:6744. [PubMed: 15869297]
28. Tomasulo M, Yildiz I, Kaanumalle SL, Raymo FM. Langmuir. 2006; 22:10284. [PubMed: 17107034]

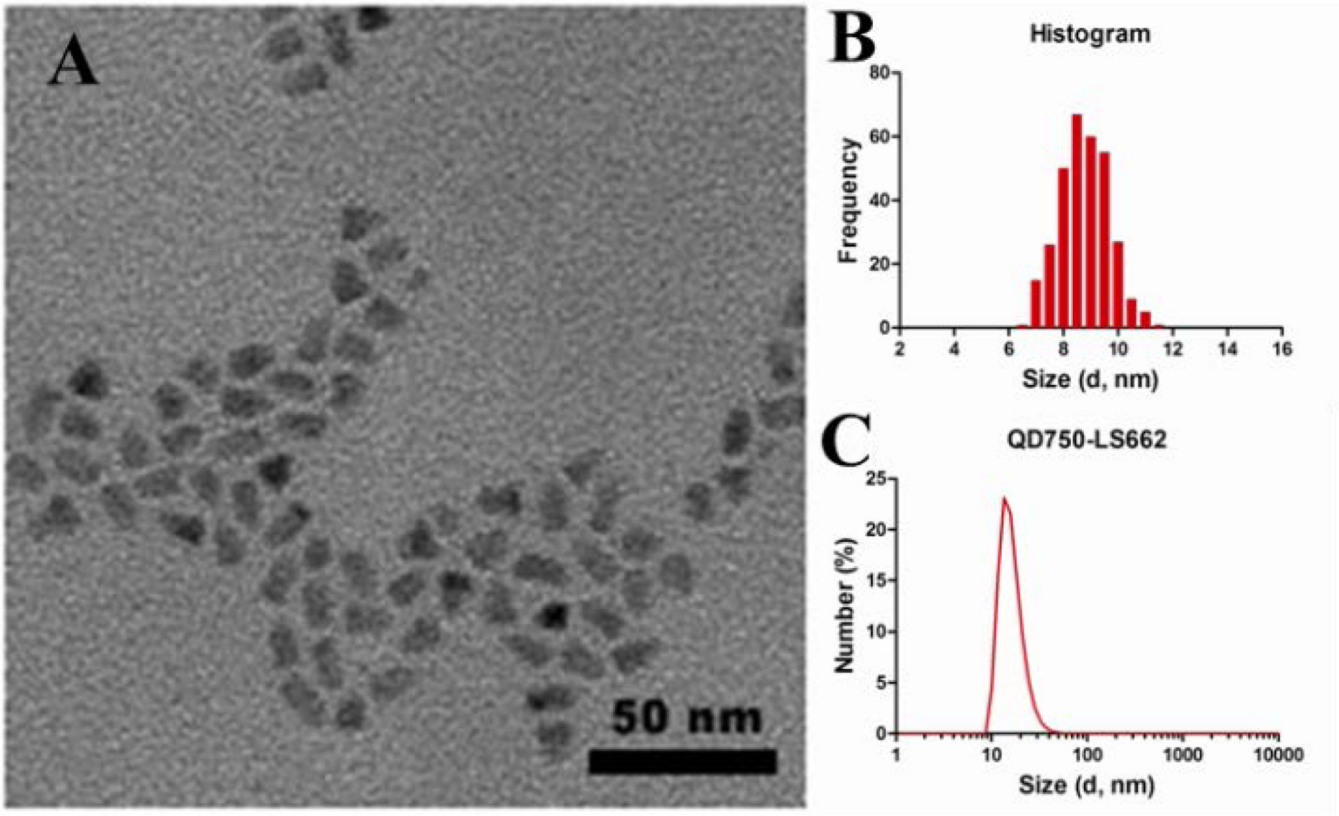

Figure 1.

(A) Representative TEM image of QD750-LS662 construct. The scale bar is 50 nm. (B) Histogram of the particle size measured from TEM images with the diameter of 9.37 nm ± 1.13 nm (±12.1%) (C) DLS measurement of QD750-LS662, showing hydrodynamic diameter of 18.17 nm ± 2.40 nm (± 13.2%).

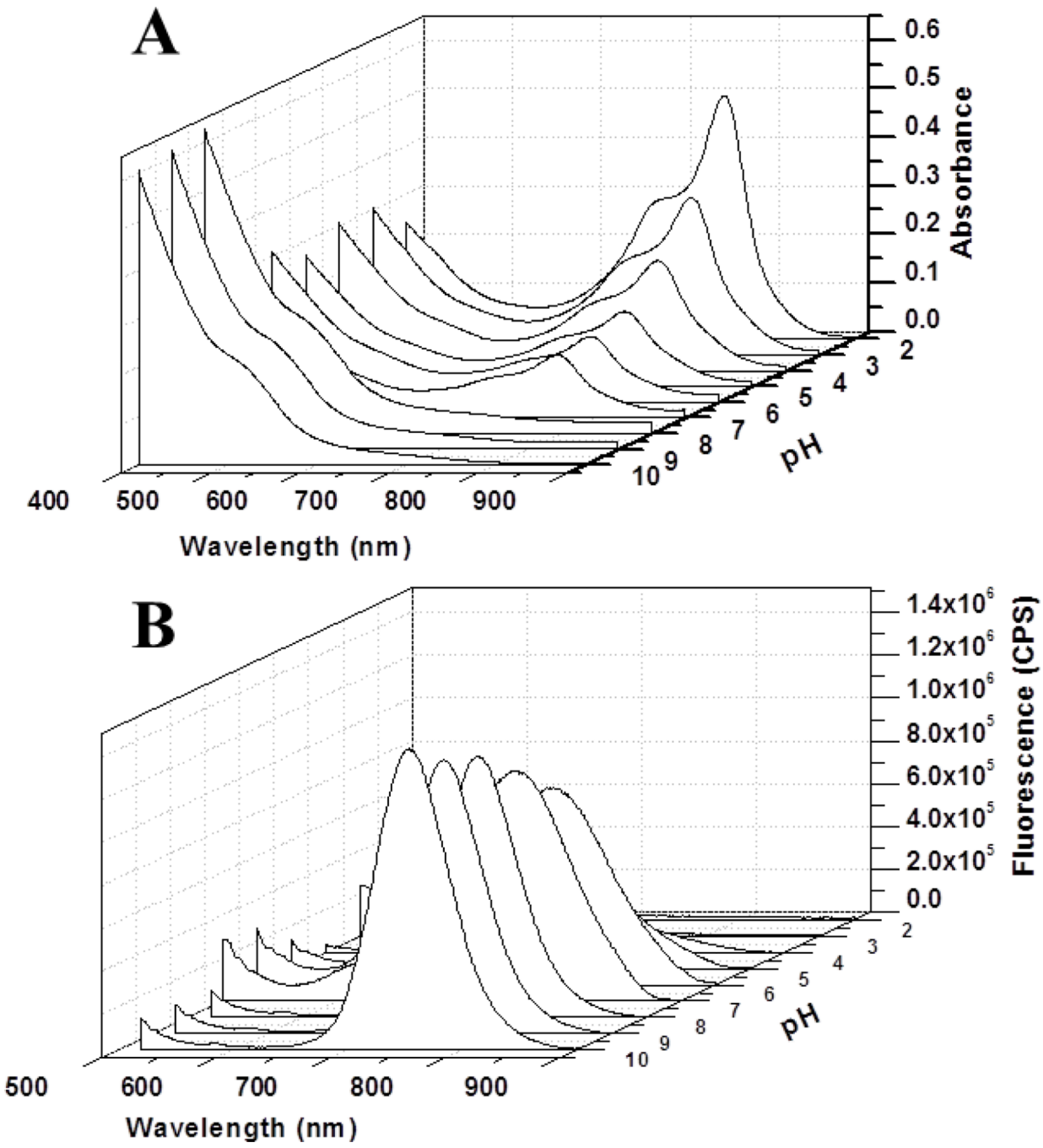

Figure 2.

(A) UV-vis absorption spectra of QD750-LS662 conjugate at different pH values. (B) Fluorescence spectra of QD750-LS662 conjugate at different pH values. The excitation wavelength is 488 nm.

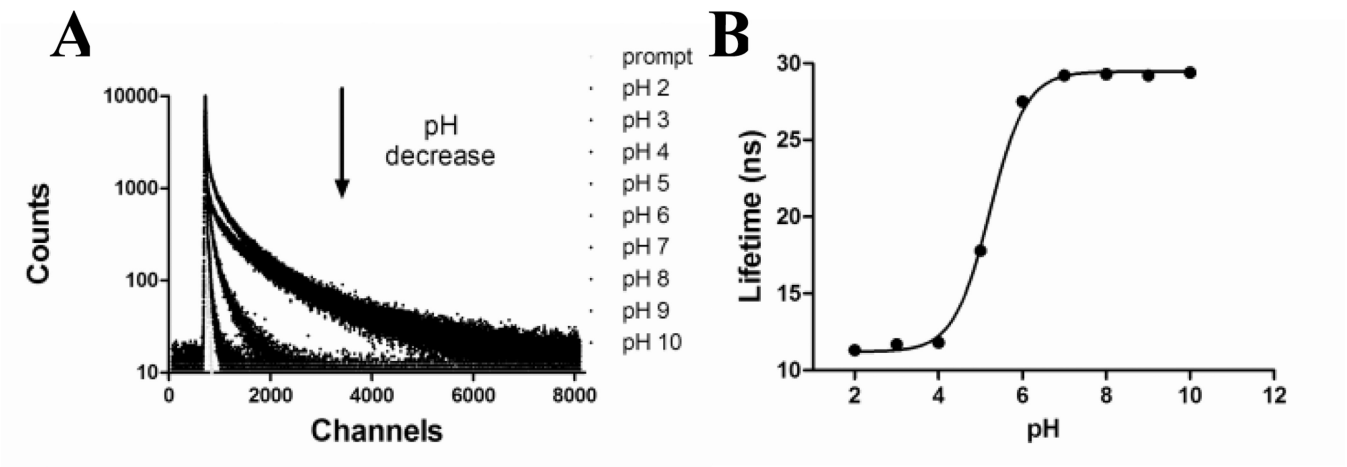

Figure 3.
(A) FLT decay profile of the QD750-LS662 conjugates at different pH values. (B) The sigmoidal fit of the FLT vs. pH, with a pKa of 5.2.

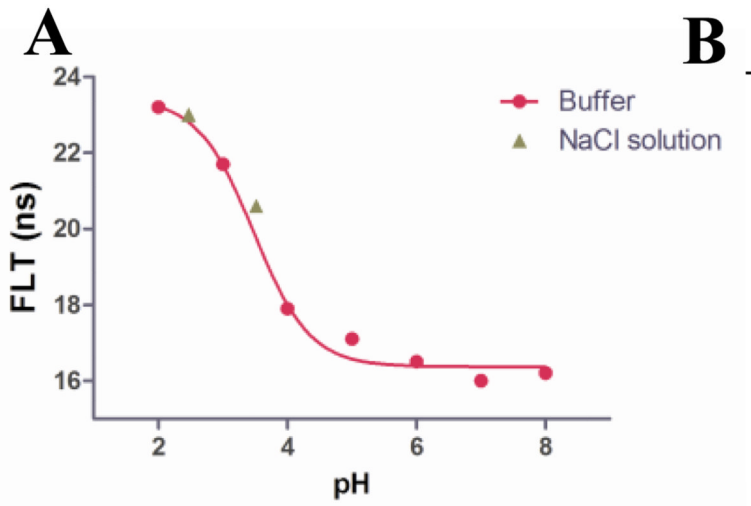

pH	Buffer	NaCl solution
2.00	23.2	
2.47		23.0
3.00	21.7	
3.52		20.6
4.00	17.9	
5.00	17.1	
6.00	16.5	
7.00	16.0	
8.00	16.2	

Figure 4.

(A) Lifetime profile of the QD760-LS664 conjugate, red solid line is the sigmoidal fit of the curve. The pKa obtained is 3.5. (B) The table of lifetime obtained from QD760-LS664 conjugate at different pH mediums; the buffer used is hydrion buffer. Two additional points are added between pH 2 and 4 by titrating 0.1M NaCl solution using HCl or NaOH to optimize the sigmoidal fit of the titration curve.

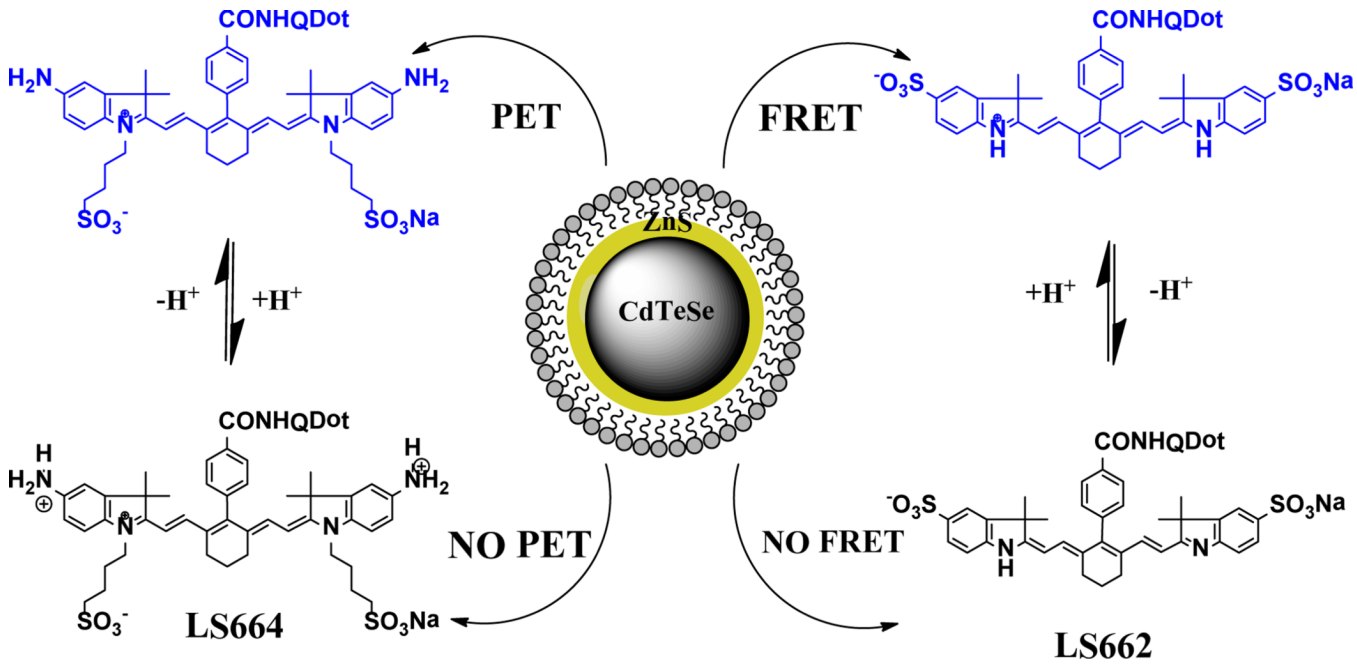

Scheme 1.
Illustration of the processes involved in the QD pH-sensing induced by pH-sensitive organic dyes.